

Shock Wave Propagation Past an Ocean Surface*

H.-T. CHEN AND R. COLLINS

*School of Engineering and Applied Science
University of California at Los Angeles, Los Angeles, California 90024*

Received May 13, 1970

The diffraction of a shock of arbitrary strength by a plane interface separating two different fluids may be calculated for the general case. The restriction encountered in earlier work on a limiting maximum difference in shock velocities in the two media has been removed by a treatment at the interface which does not depend upon Whitham's method. Instead, the shock shape at the fluid discontinuity is determined simultaneously with the local wave system to ensure continuity of both pressure and normal fluid velocity. An example is presented for the propagation of a shock front of Mach number 8 past an ocean surface. It is shown that for later times, the shock shape becomes tangent to the interface with decreasing strength there.

1. INTRODUCTION

This work generalizes the solution for the propagation of a shock front of arbitrary strength and shape into a region containing two different fluids separated by an interface parallel to the shock motion. In earlier work [1] the shape and strength of the diffracting shock wave, and the flow properties immediately behind the shock front, were determined by the method of Whitham [4]. In Whitham's method, one applies the characteristic equation, which holds along the positive characteristic behind the shock wave, to the flow quantities at the shock wave itself. Since the latter are known in terms of the shock strength from the Rankine-Hugoniot shock conditions, the substitution leads to an equation for the variation of shock strength. The solutions obtained in the earlier work [1] were limited to a maximum difference in shock velocity in the two fluids of 30%. This limitation was mainly due to the increasing contribution of secondary wave reflections at the interface for large differences in fluid properties across the free surface. In the present investigation, a generalized treatment at the interface independent of Whitham's method successfully removes this restriction. The work is considered as the first step towards the general problem of shock propagation into an

* This work was supported by the Office of Naval Research under contract N00014-69-A-0200-4013.

inhomogeneous fluid. A calculation is presented for shock propagation past an ocean surface, with shock velocities in air and water differing by approximately 250%. The jump conditions across a strong shock front in water are derived in the accompanying Appendix.

2. DIFFRACTION OF TRANSMITTED WAVE

A plane shock arrives at $t = 0$ at a contact discontinuity separating two dissimilar fluids (Fig. 1). A shock wave is transmitted into the two fluids and subsequently diffracts. A reflected wave travels upstream and is not considered here. The strength of the transmitted wave may be calculated in terms of pressure ratio across the incident shock and the sound speed and specific heat ratio in the two fluids. These details are given in Ref. [1].

The flow field behind the diffracted shock front is computed at the points of intersection of the physical characteristics $d\beta/d\alpha = \pm C$, where α and β are curvilinear axes perpendicular and tangent, respectively, to the moving shock front.

The flow field at a general point $(x_{\text{III}}, y_{\text{III}})$ at time t_{III} may then be calculated from the properties at two earlier points (x_1, y_1) and $(x_{\text{II}}, y_{\text{II}})$ in terms of the shock Mach number M , and angle of inclination θ between the local normal to the shock and the undisturbed free surface, using the following finite difference relations:

(i) Along C^+ characteristics,

$$y_{\text{III}} - y_{\text{II}} = \bar{P}_{y^+}(t_{\text{III}} - t_{\text{II}}), \quad (2.1)$$

$$x_{\text{III}} - x_{\text{II}} = \bar{P}_{x^+}(t_{\text{III}} - t_{\text{II}}), \quad (2.2)$$

$$\theta_{\text{III}} - \theta_{\text{II}} = -(M_{\text{III}} - M_{\text{II}})/\bar{N}^+; \quad (2.3)$$

(ii) Along C^- characteristics,

$$y_{\text{III}} - y_1 = \bar{P}_{y^-}(t_{\text{III}} - t_1), \quad (2.4)$$

$$x_{\text{III}} - x_1 = \bar{P}_{x^-}(t_{\text{III}} - t_1), \quad (2.5)$$

$$\theta_{\text{III}} - \theta_1 = +(M_{\text{III}} - M_1)/\bar{N}^-, \quad (2.6)$$

where

$$P_{y-} = (M \sin \theta - N \cos \theta) a, \quad (2.7)$$

$$P_{x-} = (M \cos \theta + N \sin \theta) a, \quad (2.8)$$

$$P_{y+} = (M \sin \theta + N \cos \theta) a, \quad (2.9)$$

$$P_{x+} = (M \cos \theta - N \sin \theta) a, \quad (2.10)$$

$$N = \left[\frac{K}{2} (M^2 - 1) \right]^{1/2}, \quad (2.11)$$

$$K(M) = 2 \left[\left(1 + \frac{2}{\gamma + 1} \frac{1 - \mu^2}{\mu} \right) (2\mu + 1 + M^{-2}) \right]^{-1}, \quad (2.12)$$

and

$$\mu^2 = \frac{(\gamma - 1) M^2 + 2}{2\gamma M^2 - (\gamma - 1)}.$$

The overbar indicates that the quantity has been averaged over the appropriate plus or minus characteristic.

3. COMPUTATION OF FLOW FIELD

3.1. Singularity at Interface at $t = 0$

A mathematical singularity exists at the interface at $t = 0$, since the shock velocities of the transmitted waves are discontinuous there. In order to treat

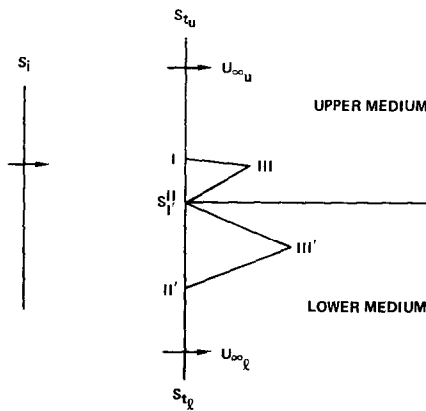


FIG. 1. Initial configuration with singularity.

the singularity, one solves the system composed of points (I, II, III) and (I', II', III') simultaneously, in terms of the Mach number and inclination angles which are unknown at the singularity (see Fig. 1).

The characteristic relations (2.1)–(2.6) simplify for $y = 0$, $t = 0$, where $\theta = 0$, $x = 0$. Equations (2.2) and (2.5) in reduced form combine to provide two relations between M and θ at the new points III and III',

$$M_{II} \cos \theta_{II} - N_{II} \sin \theta_{II} = M_I + 2N_{III} \sin \theta_{III}, \quad (3.1)$$

$$M_{I'} \cos \theta_{I'} + N_{I'} \sin \theta_{I'} = M_{II'} - 2N_{III'} \sin \theta_{III'}. \quad (3.2)$$

Four additional relations are derived from Eqs. (2.3) and (2.6) which apply both at points III and III'. The shock velocity must be continuous across the interface, and this yields a seventh relation

$$\frac{M_{II} a_{II}}{\cos \theta_{II}} = \frac{M_{I'} a_{I'}}{\cos \theta_{I'}} \quad (3.3)$$

for the eight unknowns M_{II} , θ_{II} , $M_{I'}$, $\theta_{I'}$, M_{III} , θ_{III} , $M_{III'}$, $\theta_{III'}$. The last relation must derive from the condition of continuity of pressure and velocity across the interface.

3.2. Flow Field in Interior Region

A nonlinear equation for M_{III} may be obtained by eliminating θ_{III} from Eqs. (2.3) and (2.6),

$$M_{III}(N^+ + N^-) - M_I N^+ - M_{II} N^- - (\theta_{II} - \theta_I) N^- N^+ = 0, \quad (3.4)$$

where N^\pm has been averaged along the C^\pm characteristics, respectively. The iterative solution of Eq. (3.4) yields M_{III} , and θ_{III} follows from Eq. (2.3) or (2.6).

At each new shock position, points III are calculated for a specified time t_s to facilitate location of the shock front which is a locus of points of constant time. The time t_{III} is calculated as an arithmetic mean by Eqs. (2.1) and (2.4), with P_y given by (2.7) and (2.9). If t_{III} is not equal to the prespecified time t_s , the data point farther from the free surface (point I in the upper medium or point II in the lower medium) is adjusted along the shock front and the computation repeated until t_{III} equals t_s . Ten to fifteen iterations have been found sufficient.

The calculation of interior points is continued up to the boundary with the uniform region. At the boundary, the method described above breaks down. In this case, it is necessary to fix the point farther from the interface and adjust the nearer point until convergence.

3.3. General Interface Points

Whitham's technique is not valid at the interface due to the increased importance of secondary wave reflections there.

By Lagrangian interpolation, one extends the shock front in the upper medium through the points O and I (see Fig. 2) determined from the interior calculation of the previous section and an assumed point II on the interface. The shock front

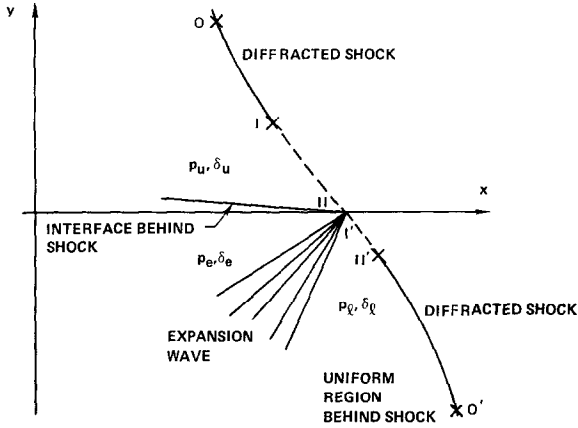


FIG. 2. Wave system for interface calculation.

is similarly extended in the lower medium through points O' and II' to the same point I'(II) on the interface. The shock inclinations θ_{II} and $\theta_{I'}$ are determined from the interpolated curves.

The shock front travels with nearly constant speed u_s along the interface [1], so that in terms of the shock coordinate x_{II} ($=x_{I'}$) at the interface,

$$u_s = \frac{x_{II}}{t_{II}} = \frac{M_{II} a_{II}}{\cos \theta_{II}} = \frac{M_{I'} a_{I'}}{\cos \theta_{I'}} \quad (3.5)$$

from Eq. (3.3). Equation (3.5) provides two relations for the solutions of M_{II} and $M_{I'}$ in terms of the specified time t_{II} ($=t_{I'} = t_s$).

The pressure and normal component of fluid velocity can be made continuous across the interface by fitting in an unsteady expansion fan at the interface behind the shock in the higher pressure medium. The details of this local expansion have been described in Ref. [1]. The continuity and momentum equations, in terms of the moving origin I' , are integrated through the expansion wave until the fluid pressure drops to the value behind the shock at the interface in the lower pressure medium. The local position of the disturbed interface is then

determined for the smallest difference in stream angles δ_u and δ_e (Fig. 2). If the stream directions are not closely matched, the interface coordinate x_{II} ($=x_1'$) must be reestimated for a minimum difference in stream angles (Golden Section Method [3]). The computation is repeated until both pressure and fluid velocity are continuous across the disturbed interface, the position of which is determined in the course of this matching procedure.

4. RESULTS AND DISCUSSION

Results are presented here for the propagation of an initially plane shock of Mach number $M_i = 8$ along an ocean surface. The strengths of the initial and transmitted shock fronts are shown in Fig. 3.

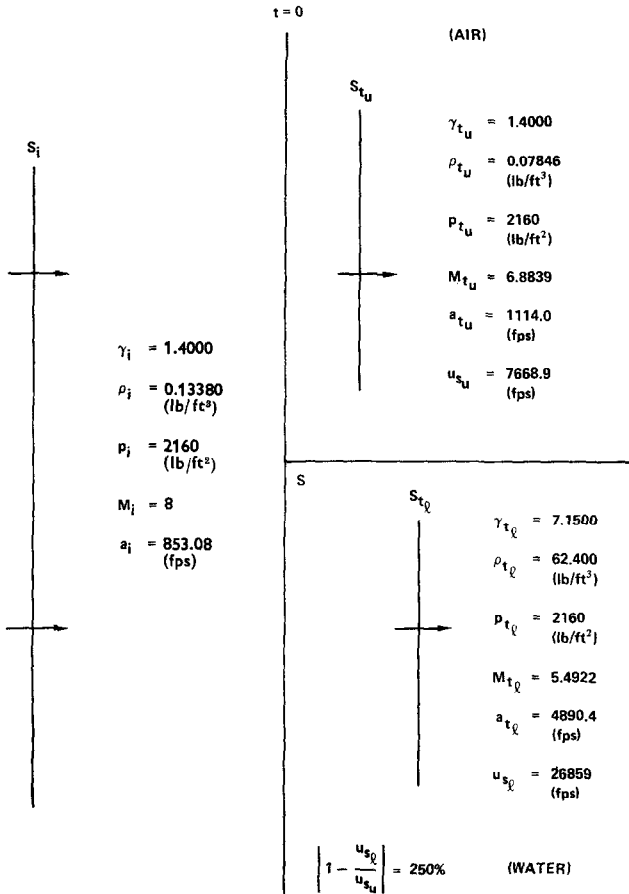


FIG. 3. Initial and transmitted shock wave at time $t = 0$ (250% difference in shock velocities).

As no characteristic length or time scale enters the problem, the shock profile must evolve from its initial shape, containing a singularity at $t = 0$, to a self-similar profile. Figure 4 shows that the shock developed in the water attains this

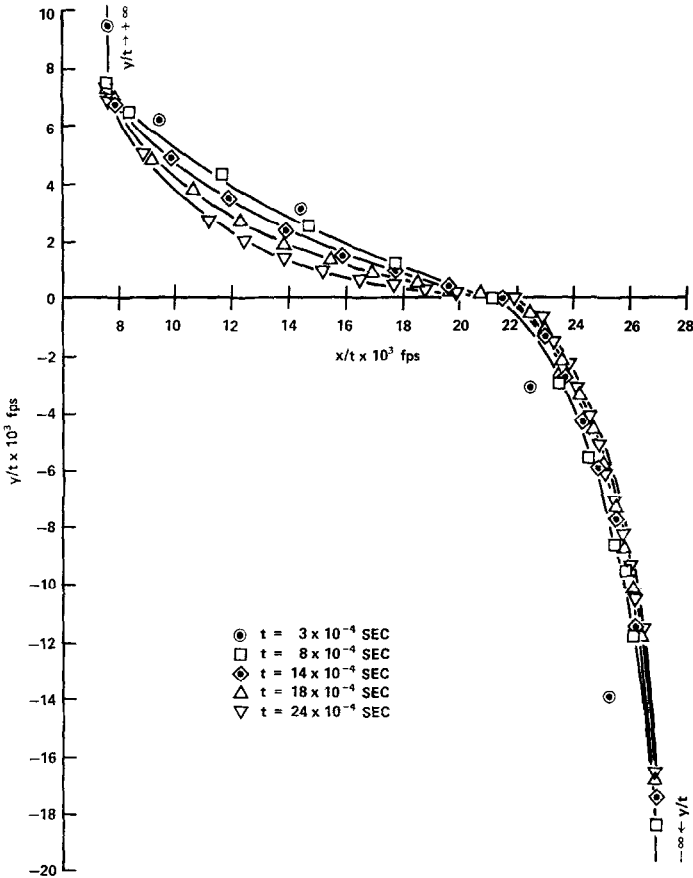


FIG. 4. Shape of diffracted shock.

invariant profile in about 8×10^{-4} sec, with longer times required in the air. In the neighborhood of the interface, the air shock approaches the tangent to the free surface, with an almost constant velocity of propagation along the interface (Fig. 5) of approximately 21,000 ft/sec during the time interval 25×10^{-4} sec.

The variation in pressure behind the shock is plotted in Fig. 6. The water shock appears to exhibit smaller changes in curvature than the air shock. Accordingly,

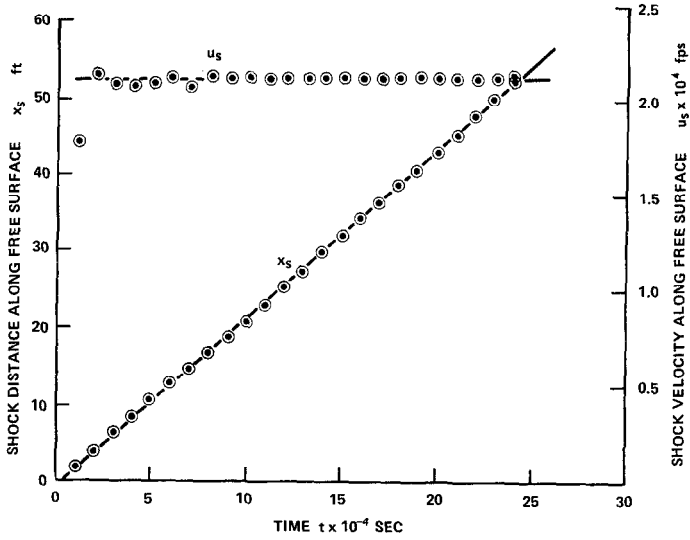


FIG. 5. Shock propagation along an ocean surface.

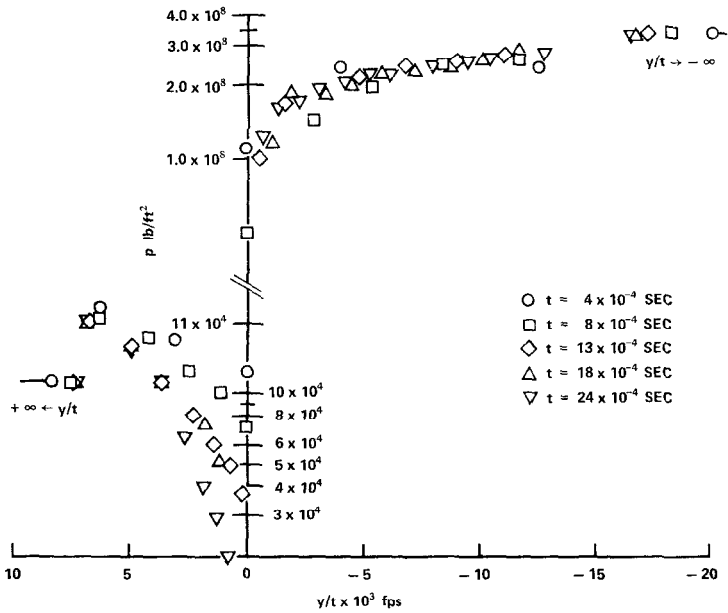


FIG. 6. Pressure variation behind diffracted shock.

the pressure distribution behind the shock in the water shows a threefold variation, with a minimum of 10^8 lb/ft² occurring at the interface. The air shock however, is much more distorted with a corresponding 30-fold pressure variation from 12.2×10^4 lb/ft² behind the uniform shock to a minimum of 0.43×10^4 psi

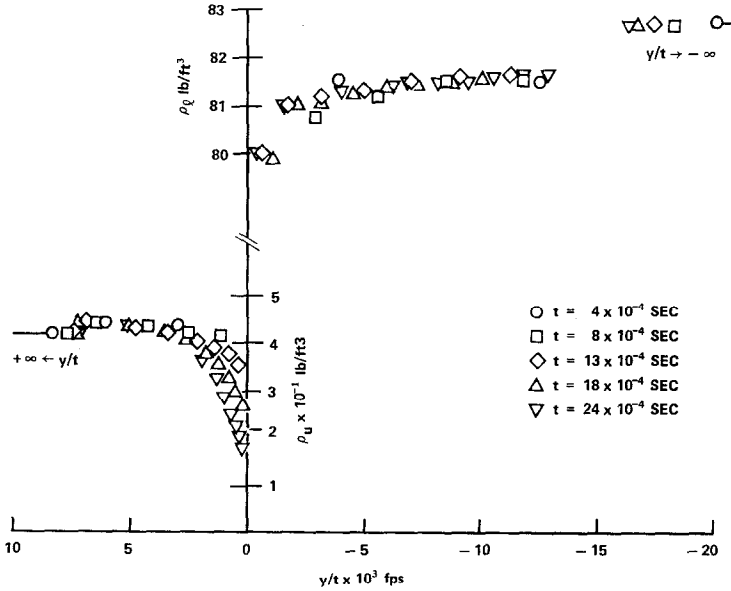


FIG. 7. Variation of fluid density behind diffracted shock.

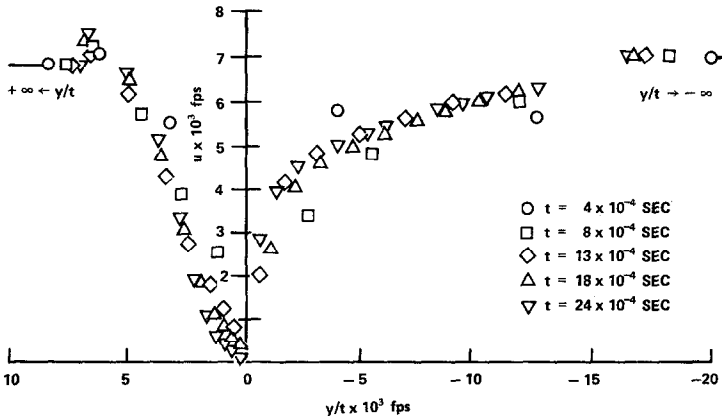


FIG. 8. Horizontal component of fluid velocity behind shock.

TABLE I
Pressure and Inclination of Ocean Surface Behind Shock

t (10^{-4} sec)	δ_u (degrees)	δ_e (degrees)	P_u (10^3 lb/ft 2)	P_e (10^3 lb/ft 2)
0	14.378	14.386	403.14	403.14
5	16.445	16.472	106.65	106.69
10	11.194	11.190	54.643	54.643
15	7.2101	7.2240	25.782	25.737
20	3.7119	3.7032	9.8673	9.8330
24	1.5060	1.5097	4.2891	4.2891

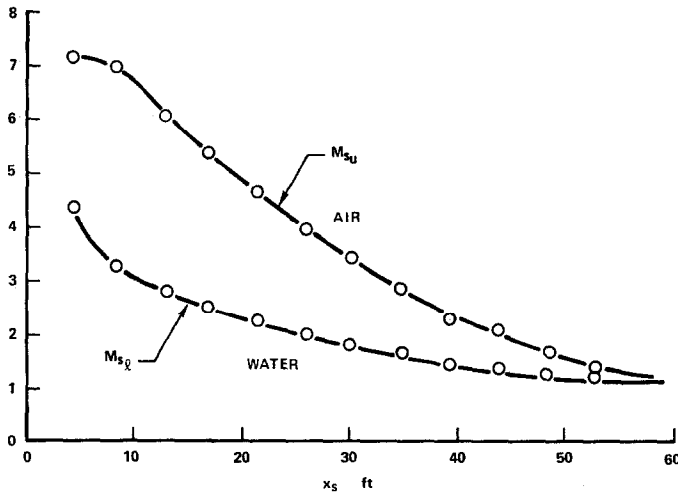
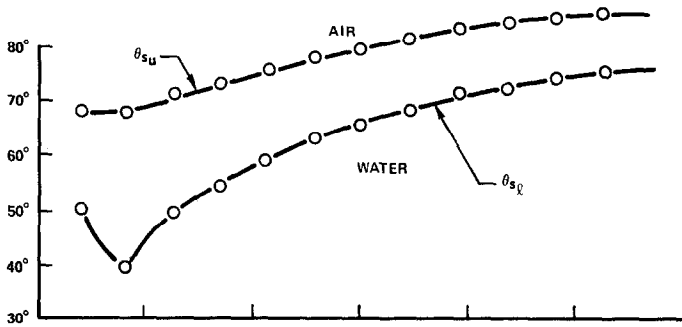


FIG. 9. Variation of shock inclination and Mach number along ocean surface.

at the interface. An expansion fan develops to render the pressure continuous across the free surface.

The fluid density (Fig. 7) is almost constant in the water at 81.5 lb/ft³ and drops to a sharp minimum at the interface under the influence of the expansion fan. The air density falls from a value of approximately 0.45 lb/ft³ behind the uniform shock to a minimum of 0.15 lb/ft at the free surface.

The horizontal component of fluid velocity behind the shock is plotted in Fig. 8. An expansion fan behind the shock at the free surface assures continuity of streamline direction at $y = 0$.

The conditions of continuity of pressure p and stream angle δ have been satisfied at each point along the air-water interface as the shock passes. Table I indicates the very close agreement on both sides of the interface.

The shock front decreases rapidly in strength near the ocean surface. Although the air and water shocks join at the interface, nonetheless, the local slopes are discontinuous there. The shock inclination and shock Mach number are shown for both the air and water in Fig. 9 as a function of shock distance along the ocean surface. Apparently these values approach a constant limit asymptotically for distance along the ocean surface in excess of 50 ft.

At the free surface itself, the shock angle in the air approaches the tangent to the surface. In order to maintain the same velocity $M_{sa}/\cos \theta$ past the surface,

TABLE II

Shape, Strength, and Inclination Angle of Shock

t (10^{-4} sec)	x (ft)	y (ft)	M	θ (degrees)
4	3.0676	3.3400	6.8839	0
4	5.8364	1.2209	7.8682	55.128
4	8.2722	0.0	3.2674	39.406
4	9.6062	-2.3910	4.7680	14.007
4	10.744	-8.3460	5.4922	0
13	9.9695	9.7358	6.8839	0.0
13	23.732	1.0131	4.3397	74.424
13	28.943	-0.96134	3.5210	45.720
13	31.091	-4.1948	4.3077	24.417
13	34.917	-22.428	5.4922	0.0
24	18.405	17.289	6.8839	0.0
24	45.082	0.75048	1.8703	82.716
24	52.554	0.0	1.1317	75.360
24	56.934	-5.5412	4.2285	26.250
24	64.462	-39.640	5.4922	0.0

it is necessary for the shock Mach number M_s to decrease. This accounts for the greatly reduced shock strength observed at the ocean surface.

Table II shows the calculations of shape, strength, and inclination angle of the diffracted shock at selected times.

APPENDIX. SHOCK CONDITION IN WATER

Denoting shock velocity by U and fluid velocity by u , the conservation of mass, momentum, and energy across a plane normal shock may be expressed, respectively, as

$$\rho_0 U = \rho(U - u), \quad p - p_0 = \rho_0 U u, \quad e - e_0 = (p_0 + p)(\rho - \rho_0)/2\rho\rho_0, \quad (\text{A.1})$$

in terms of density ρ , pressure p , and internal energy e , where the zero subscript refers to upstream conditions.

From the first two relations, one determines the shock and fluid velocities as

$$U = \{\rho(p - p_0)/\rho_0(\rho - \rho_0)\}^{1/2}, \quad u = \{(p - p_0)(\rho - \rho_0)/\rho\rho_0\}^{1/2}. \quad (\text{A.2})$$

The equation of state of water at high pressure has been given by Tamman [2] in terms of temperature T as

$$(p + p_c)/\rho = KT, \quad (\text{A.3})$$

where $p_c = 3000$ atm, $K = 6690$ ft-lb/°R.

The internal energy of water is

$$e - e_0 = \bar{C}_v(T - T_0) + p_c \left(\frac{1}{\rho} - \frac{1}{\rho_0} \right), \quad (\text{A.4})$$

where \bar{C}_v is an average specific heat at constant volume given by

$$\bar{C}_v = \int_{T_0}^T \frac{C_v}{T - T_0} dT \quad (\text{A.5})$$

Temperature T may be eliminated from Eqs. (A.3) and (A.4) to yield

$$e - e_0 = \bar{C}_v/K \{ (p + p_c)/\rho - (p_0 + p_c)/\rho_0 \} + p_c \left(\frac{1}{\rho} - \frac{1}{\rho_0} \right). \quad (\text{A.6})$$

The internal energy may be eliminated between (A.4) and the energy equation of (A.1) to give the Rankine-Hugoniot relation for water,

$$\begin{aligned} \frac{\rho_0}{\rho} &= \frac{[2(\bar{C}_v/K) + 1](p_0 + p_c)/(p + p_c) + 1}{[2(\bar{C}_v/K) + 1] + (p_0 + p_c)/(p + p_c)} \\ &= \frac{(\gamma + 1)\xi + (\gamma - 1)}{(\gamma - 1)\xi + (\gamma + 1)}, \end{aligned} \quad (\text{A.7})$$

where

$$\xi = \frac{p_0 + p_c}{p + p_c}, \quad \gamma = 1 + \frac{K}{\bar{C}_v} \simeq 7.15.$$

Equation (A.7) reduces to the shock condition for an ideal gas if $p_c = 0$, and to the well-known Tait equation for water if the flow is isentropic. Equation (A.2) then yields the shock and fluid velocities in water.

REFERENCES

1. R. COLLINS AND H.-T. CHEN, Propagation of a shock wave of arbitrary strength in two half planes containing a free surface, *J. Comp. Phys.* **5** (1970), 555.
2. G. TAMMANN, *Ann. Phys.* **37** (1917), 975.
3. D. J. WILDE, "Optimum Seeking Methods," pp. 30-40, Prentice-Hall, Englewood Cliffs, N. J., 1964.
4. G. B. WHITHAM, On the propagation of shock waves through regions of non-uniform area or flow, *J. Fluid Mech.* **4** (1958), 337-360.